Mechanism of Glidants: Investigation of the Effect of Different Colloidal Silicon Dioxide Types on Powder Flow by Atomic Force and Scanning Electron Microscopy

S. JONAT,[1] S. HASENZAHL,[2] A. GRAY,[2] PETER CHRISTIAN SCHMIDT[1]

[1]Department of Pharmaceutical Technology, University of Tübingen, 72076 Tübingen, Germany

[2]Degussa AG, Technical Service Aerosil, 63457 Hanau-Wolfgang, Germany

Received 13 January 2004; revised 26 May 2004; accepted 27 May 2004

Published online in Wiley InterScience (www.interscience.wiley.com). DOI 10.1002/jps.20172

ABSTRACT: The effect of hydrophilic and hydrophobic colloidal silicon dioxide types (CSD) on the flow characteristics of microcrystalline cellulose (MCC) under different mixing conditions was macroscopically measured using the angle of repose method, the bulk and tapped densities. CSD ameliorated the flow characteristics in general, but hydrophobic CSD was more effective compared to the hydrophilic types under gentle mixing conditions. The macroscopic effect was explained on the particle level by scanning electron (SEM) and atomic force microscopy (AFM) studies. The CSD distribution on the MCC surface was more uniform for the hydrophobic type and was independent from the mixing conditions used in this study. From the cumulative adhesion force distributions of the mixtures, determined by AFM, the mean and the standard deviation of the adhesion force were calculated. The means were 44.8 nN for MCC alone, 25.2 and 28.3 nN for mixtures containing the two hydrophilic types, and 13.8 N for the hydrophobic CSD under gentle mixing conditions in a Turbula mixer. Stronger mixing in a plowshare mixer led to a further reduction to 17.5 and 17.4 nN for the two hydrophilic types, while the hydrophobic CSD showing a value of 13.9 nN was unchanged. A linear correlation between the angle of repose and the adhesion force could be established, indicating that for routine measurements of the efficiency of a glidant the simple angle of repose method is sufficient. J Pharm Sci 93:2635–2644, 2004

Keywords: atomic force microscopy; scanning electron microscopy; angle of repose; powder technology; mixing; adhesion; microcrystalline cellulose; colloidal silicon dioxide

INTRODUCTION

Powder mixing as a unit operation in the manufacture of solid dosage forms determines not only the technological properties of the mixture but also the content uniformity of the active ingredient.[1–6] From a technological point of view, the homogeneity of low dosed excipients like magnesium stearate and colloidal silicon dioxide (CSD) is of importance.[7,8] They are added to cohesive powders or granules and must be uniformly distributed to fulfill their lubricant or glidant function. Powder processing is also of major importance for the uniform distribution of CSD. The primary particles of CSD are linked into relatively stable aggregates that can range up to several hundred nanometers in size, which in turn form larger agglomerates. Mixing conditions strongly influence the size and distribution of the agglomerates and aggregates and as a result the flowability of the powder mixture. Sindel et al.[9] examined the

Correspondence to: Peter Christian Schmidt (Telephone: +49(0)70712978462; Fax: +49(0)7071295531; E-mail: peter-christian.schmidt@uni-tuebingen.de)

Journal of Pharmaceutical Sciences, Vol. 93, 2635–2644 (2004)

homogeneity of a mixture of CSD and lactose by measuring the angle of repose and by determining the variance of the CSD content. At the optimum mixing time, a significant reduction of the angle of repose was found.

Physical test methods for powder flow characterization described in the literature are numerous.[10,11] For this study, the classical angle of repose, bulk and tapped densities[12] were chosen to evaluate the action of CSD on microcrystalline cellulose (MCC) on a macroscopic level. To characterize the glidant action, complementary investigations were performed to visualize the degree of CSD particle (aggregates and agglomerates) coverage and distribution on the MCC surface and to determine the interparticulate forces within the powder mixture. Previously used techniques for the determination of interparticulate forces include the vibration method, the centrifuge technique, and the impact separation method.[13] These methods determine the adhesion force by measuring the amount or number of drug particles that detach from a surface at a given force. Atomic force microscopy (AFM) is an alternative technique whereby the adhesion force is determined using single particle detachment.

AFM was developed by Binning et al.[14] in 1986 to overcome the limitations of scanning tunnelling microscopy in achieving atomic resolution of metals and semiconductors. It enables high-resolution topographical imaging of surfaces and records fundamental properties of sample surfaces. By mounting a particle to a cantilever, AFM permits the measurement of forces between this specific particle and a substrate surface. For this purpose, the probe particle is glued to the end of a microfabricated cantilever and the substrate is attached to the flat surface on the AFM piezoelectric transducer, which is used to change the relative position between the particle and the substrate. The cantilever deflection is recorded as it interacts with the moving substrate and is converted into an interaction force. A schematic diagram of and complementary information on AFM can be found in the literature.[15,16] Interaction forces can be studied over a wide range of environmental conditions such as temperature, humidity, and gas atmosphere.

AFM has paved the way for new experiments. The applications are numerous and concern various fields, for example, physics, biophysics, biochemistry, microelectronics, and metallurgical engineering.[17–20] Recently, AFM has found application in the pharmaceutical field for evaluating the surface or the adhesional properties of carriers,[15,21,22] drug substances,[24,25] or in determining their interaction.[26,27] Additional studies have been reported in other pharmaceutical fields. Ibrahim et al.[23] measured the adhesion force of individual lactose particles to the surface of gelatine capsules, while Wang et al.[28] used AFM to model adhesion phenomena in tablet compression. Ohta et al.[29] and Weth et al.[30] used AFM to investigate glidants and correlated the attractive forces with the powder flow.

The purpose of the present investigation was to compare the flow-enhancing properties of different types of CSD on MCC with respect to mixing conditions and to explain the changes in the powder flow characteristics by scanning electron microscopy (SEM) and AFM.

MATERIALS AND METHODS

Materials

AEROSIL® 200, a hydrophilic and non-compacted CSD, AEROSIL® 200 VV Pharma and AEROSIL® 130 V, two hydrophilic and compacted CSDs, AEROSIL® R 972 V and AEROSIL® R 974 V, two hydrophobic and compacted CSDs were used as received from Degussa AG (Düsseldorf, Germany). Their physico-chemical properties are listed in Table 1.[31]

AEROSIL® 130 and AEROSIL® 200 are the starting materials for the synthesis of AEROSIL® R 972 V and AEROSIL® R 974 V, respectively.

MCC (Avicel® PH 101, FMC Biopolymer, Cork, Ireland) was used as supplied.

Preparation of Mixtures

Based on preliminary investigations, the CSD concentration was set to 0.5% w/w. CSD was prescreened through a 315 μm sieve onto a portion of the MCC. The remaining portion of MCC was added and mixed by hand. The mixture was sieved through an 800 μm sieve before and after 10 min mixing in a free-fall mixer (Turbula T2C, W. A. Bachofen, Basel, Switzerland) with a 2 L vessel, a maximum filling degree of 75% and a rotational speed of 42 rpm. The resulting mixture was named M1. A second batch of mixture M1 was prepared and mixed an additional 10 min in a high speed mixer based on the plowshare principle (SW 1/S, Erweka, GmbH, Heusenstamm, Germany) to produce mixture M2.

Table 1. Physicochemical Properties of Hydrophilic and Hydrophobic Colloidal Silicon Dioxide (CSD) Types Used in This Study

	AEROSIL® 200	AEROSIL® 200 VV	AEROSIL® 130 V	AEROSIL® R 972 V	AEROSIL® R 974 V
Average primary particle size (nm)[a]	12	12	16	16	12
BET surface area (m^2/g)[b]	206	201	138	111	176
Bulk density (g/cm^3)[b]	0.050	0.119	0.104	0.094	0.089
Tapped density (g/cm^3)[b]	0.054	0.134	0.118	0.115	0.105
Silanol group density (nm^{-2})[a]	Approximately 2	Approximately 2	Approximately 2	Approximately 0.75	Approximately 0.75
Behavior towards water	Hydrophilic	Hydrophilic	Hydrophilic	Hydrophobic	Hydrophobic

[a]Typical values.
[b]Batch record, ex-plant.

Physical Characterization

Bulk density was measured using a plastic powder funnel (run out diameter 3 cm). Approximately 150–200 mL of mixture corresponding to 70.0 g of powder mixture were filled into a tared 250 mL graduated cylinder (base diameter 6 cm). The cylinder containing the product was weighed to ±0.1 g (model PG 4002-S, Mettler Toledo GmbH, Giessen, Germany) and the volume was read to ±1 mL. The bulk density was calculated as g/cm^3. Three samples per lot were tested for the mixtures. The values from CSD were obtained from batch records. After measuring the bulk density, the filled cylinder was placed in a settling apparatus (model STAV 2003, J. Engelsmann AG, Ludwigshafen, Germany) and tapped 1250 or 2500 times. The final volume was recorded to ±1 mL and the tapped density was calculated in g/cm^3 using the weight obtained during the bulk density measurement. Three samples per lot were tested for the mixtures. The values from CSD were obtained from batch records.

The specific surface area was determined by nitrogen gas adsorption at a temperature of 77 K according to ISO Norm 9277 (based on the BET method) for disperse, nonporous solids. Samples were first prepared by drying overnight at 105°C, followed by degassing for 1 h at 200°C *in vacuo* before performing the analysis using the volumetric method (Model ASAP 2400, Micromeritics, Norcross, GA). Six data points were recorded for $0.05 < p/p_0 < 0.22$.

The particle size distributions of Avicel® PH 101 was measured by laser diffraction spectrometry (Mastersizer 2000, Malvern Instruments GmbH, Herrenberg, Germany) using the dry-dispersing system Scirocco 2000 (Malvern Instruments GmbH). The dispersing air pressure was 3 bar. Data were collected directly by means of the system software (Malvern Instruments GmbH). The mean value of three measurements was calculated.

The angle of repose of the mixtures was measured using a sieve-cone-method according to DIN ISO 4324. The distance between the sieve and the metal cylinder was kept at 10 cm. First, 100 g of material were sieved through an 800 μm sieve onto a metal cylinder with a radius (r) of 25 mm to determine the exact distance between the cone and the sieve. The sieve was then fixed 3 cm above the top of the powder cone, the cylinder surface was cleaned, and 100 g of material were sieved through an 800 μm sieve onto the metal cylinder. The height (h) of the powder cone was measured with digital counter type height gage (model 192-106, Mitutoyo Meßgeräte GmbH, Neuss, Germany) with a 0.03 mm accuracy. The angle of repose (α) was calculated using the following equation: $\tan \alpha = h/r$. The mean, the standard deviation and the 95% confidence interval of six samples were calculated.

The MCC surface was examined by SEM using a Zeiss DSM 940 A instrument (Carl Zeiss, Oberkochen, Germany) equipped with a Contax M 167 MT camera (Yashica-Kyocera, Hamburg, Germany). Each mixture was fixed on an aluminium pin using double-adhesive tape (Tempfix) and then coated with a thin gold layer prior to examination using a Sputter Coater E 1500 (Bio-Rad, Munich, Germany). The samples were sputtered four times for 60 s and exposed to 20 mA current and 2.1 kV acceleration voltage at a vacuum of 0.02–0.03 mbar. The micrographs were taken at 5 kV and at magnifications of 5000 and 20000.

AFM

Sample Preparation

Powder samples for adhesion measurements were prepared immediately before use. Samples of bulk MCC and mixtures M1 and M2 containing AEROSIL® 200, AEROSIL® 200 VV, and AEROSIL® R 972 V were immobilized on an AFM stub using a doubled-sided adhesive tape. Excess loose powder was removed. The mean particle diameter of Avicel® PH 101 particles, determined by laser diffraction spectroscopy, was 48.8, 49.5, and 49.7 μm for MCC as bulk, and after mixing conditions 1 and 2, respectively.

Cantilever Preparation

A selected small and almost isometric MCC particle (10 μm in size determined using an optical microscope) was attached to the apex of an oxide-sharpened silicon nitride cantilever (Type NP-20, Digital Instruments, Veeco Inst., Santa Barbara, CA) with a small quantity of epoxy resin (UHU plus endfest 300, UHU GmbH & Co., KG, Bühl, Germany) under an optical microscope (Ergolux, Ernst Leitz, Wetzlar, Germany). Care was taken to prevent the spreading of epoxy resin around the cantilever and the particle. The MCC functionalized cantilever was examined under an optical microscope after drying overnight to ensure the successful attachment of the MCC particle and also after each measurement to ensure the particle integrity.

The cantilever spring constant ($k = 0.23$ N/m) was determined using a dynamic method as described by Cleveland.[32] A glass sphere of known mass was attached to the end of the cantilever and the change in resonance frequency was measured. The glass sphere adhered naturally and could be easily removed before using the cantilever, making the method non-destructive.

Adhesion Measurements

Adhesion measurements were performed in air at room temperature (20–25°C) and ambient relative humidity (40–50% RH) using an atomic force microscope (Multimode SPM, Digital Instruments). All force–distance measurements were recorded with the following settings: 6 μm approach-retraction cycle and 1 Hz cycle rate. A digital camera (Coolpix 990, Nikon) was used to locate the MCC functionalized cantilever on top of an individual MCC particle from the sample. The adhesion force distribution was obtained from adhesion measurements of at least 50 individual sites for mixtures M1 and M2 and 30 sites for MCC. Ten force plots were captured at each site. The force–distance plot of the atomic force microscope is well-described in the literature.[20,26,33] The adhesion force (F) was calculated according to Hook's law, $F = kx$, where k is the spring constant and x is the vertical displacement of the cantilever. For an accurate adhesion force calculation, the vertical displacement was recorded using a piezoscanner that measures the difference in distance (Δz) between the point at which the probe, in contact with the surface, crossed the zero deflection line, and the point at which the probe pulled free from the surface.[34]

RESULTS AND DISCUSSION

Powder Flow Characterization

The flowability test using a standard funnel could not be performed because Avicel PH 101 without CSD did not flow through the funnel. The angle of repose of the mixtures, which as reported in our previous study,[35] correlated well to the measurement of flow rate using a dynamic conveyor belt method, was then measured using a sieve-cone-method. The flow characteristics were differently affected by the mixing conditions although the particle size of MCC remained unchanged (49.5 and 49.7 μm for MCC after mixing conditions 1 and 2, respectively). The mixing condition did not significantly influence the powder flow characteristics of mixtures containing MCC without CSD, namely the angle of repose, the bulk and tapped densities (Table 2).

Each CSD-type increased the bulk density to the same extent and the values ranged from 0.389 to 0.416 g/cm^3. Therefore, the density of the powder cone resulting during the angle of repose measurements of mixtures containing CSD was not influenced by the different CSD-types and the mixing conditions. The interparticle distance between MCC particles was the same for all MCC–CSD mixtures. As expected, the addition of CSD decreased the angle of repose of MCC under both mixing conditions (Fig. 1). The small spherical CSD agglomerates adhered to the surface of MCC and reduced the attraction forces between two MCC particles. MCC mixtures containing hydrophobic CSD-types exhibited lower angles of repose compared to mixtures containing hydrophilic CSD-types, resulting in better flow properties at very similar interparticle distance. Moreover,

Table 2. Angle of Repose ($n = 6$), Bulk and Tapped Densities ($n = 3$) of the Different CSD Types–Microcrystalline Cellulose (MCC) Mixtures at Mixing Conditions 1 and 2

	MCC		AEROSIL® 200		AEROSIL® R 200 VV		AEROSIL® 130 V		AEROSIL® R 972 V		AEROSIL® R 974 V	
	M1	M2	M1	M2	M1	M2	M1	M2	M1	M2	M1	M2
Angle of repose (°)	46.8	47.3	40.7	37.2	39.2	37.1	40.5	38.1	35.7	35.7	36.3	35.5
Bulk density (g/cm^3)	0.356	0.357	0.389	0.4	0.404	0.407	0.394	0.402	0.416	0.411	0.411	0.407
Tapped density (g/cm^3)	0.457	0.455	0.468	0.51	0.471	0.508	0.476	0.5	0.518	0.518	0.519	0.524

mixtures containing hydrophilic CSD were influenced by the mixing conditions. The angle of repose decreased (by 5.5–8.7%), i.e., the flowability increased, under forced mixing conditions in the plowshare mixer. By contrast, the mixtures M1 and M2 containing hydrophobic CSD showed no statistically significant differences in the angles of repose and therefore seemed to be independent from the mixing steps.

Addition of CSD increased the tapped density of MCC. The CSD particles adhering to the MCC surface reduced the interparticle forces between the MCC and increased the roller friction compared to the sliding friction. During tapping, the MCC particles moved closer to each other and reduced the space between them. The same influence of the CSD and the mixing conditions was previously observed with the angle of repose. Figure 2 is the mirror image of Figure 1. The addition of hydrophobic CSD showed higher tapped densities compared to the addition of hydrophilic CSD and was not influenced by the mixing conditions (Fig. 2 and Table 2).

The primary particle size of the CSD type cannot be held responsible for these differences because AEROSIL® 200 VV and AEROSIL® 130 V have the same primary particle sizes as AEROSIL® R 974 V and AEROSIL® R 972 V, respectively (Table 1). Additionally, no dependence of the angle of repose on CSD surface area and tapped density was observed. The results indicate that other factors like surface chemistry influence the glidant properties of different CSD types.

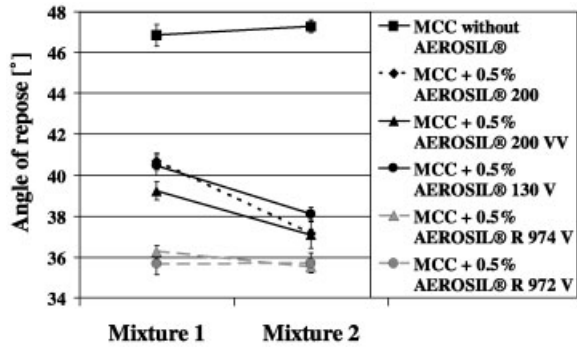

Figure 1. The effect of colloidal silicon dioxide (CSD) and mixer type on the angle of response of microcrystalline cellulose (MCC) mixtures. Error bars indicate the 95% confidence interval of six measurements.

SEM

In order to analyze and to elucidate the aforementioned differences between different CSD types, SEM images were taken to visualize the degree of CSD particle coverage and distribution on the MCC surface. This study included AEROSIL® 200, a conventional and commonly used CSD, AEROSIL® 200 VV, a new compacted hydrophilic CSD, and AEROSIL® R 972 V, a new compacted hydrophobic CSD. SEM-samples were carefully checked to make sure that the differences observed were representative for each particular mixture. The comparison of Figure 3a,c,e, shows that the MCC surface was covered with small particles of CSD (aggregates and agglomerates), however, to varying degrees. The distribution of hydrophobic CSD on the surface of MCC

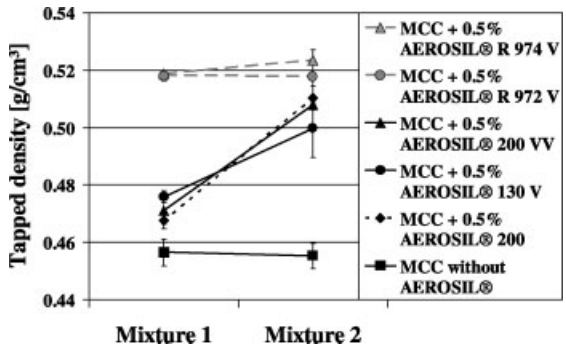

Figure 2. The effect of CSD and mixer type on the taped density of MCC mixtures. Error bars indicate the 95% confidence interval of three measurements.

was regular, uniform, and homogeneous without enrichment of CSD particles at the edges or in cavities (Fig. 3a). Additional mixing M2 (Fig. 3b) did not influence the degree and uniformity of coverage of hydrophobic CSD. Although the proportion of CSD in the mixture was the same for every sample, the coverage of MCC was less extensive and the distribution was less homogeneous for mixtures containing hydrophilic CSD (Fig. 3c,e). Furthermore, large CSD particles were observed on the MCC surfaces or in cavities, indicating that the CSD agglomerates were not sufficiently broken up under mixing conditions 1. Figure 3d,f show that higher energy mixing conditions were necessary to achieve a homogeneous distribution of hydrophilic CSD particles. The degree of coverage qualitatively correlated to the flow-enhancement. A higher degree of coverage allowed a better action of the glidant particles.

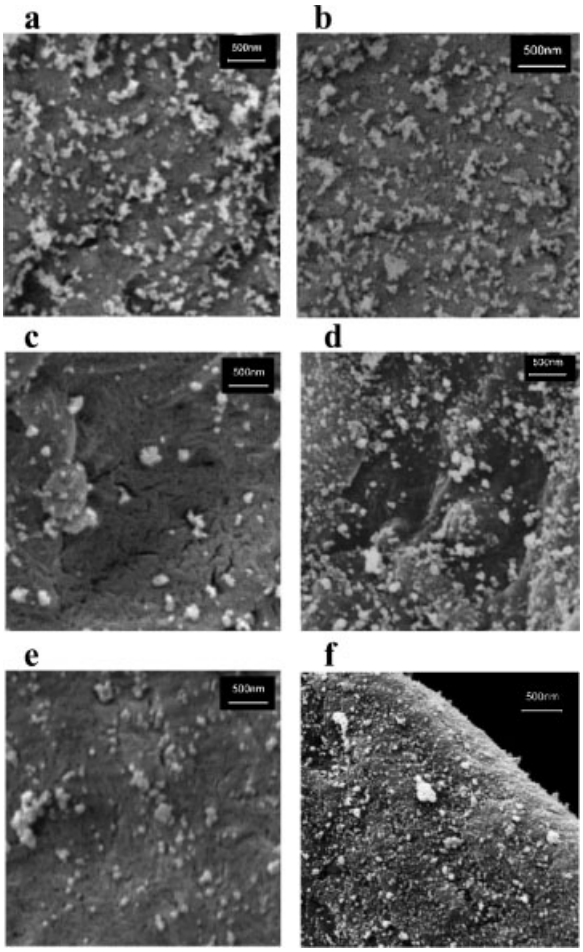

Figure 3. Scanning electron microscopy (SEM) images of MCC containing 0.5% AEROSIL® R 972 V [M1, (a); M2, (b)], 0.5% AEROSIL® 200 [M1, (c); M2, (d)], and 0.5% AEROSIL® 200 VV [M1, (e); M2, (f)]. The bar represents 500 nm.

This SEM analysis indicated that the degree and uniformity of coverage of the CSD on the MCC surface plays a key role in the reduction of the angle of repose. This observation can be explained by the nature of the CSD. Primary particles of CSD are linked into relatively stable aggregates, which in turn form larger agglomerates. The prevailing forces within the agglomerates are hydrogen bonds. By reacting the silanol groups with organosilicon compounds to create hydrophobic CSD, the density of silanol groups of hydrophobic CSD decreases as shown in Table 1. Consequently the hydrogen bonds within the agglomerates are fewer, leading to softer agglomerates compared to the hydrophilic types. Agglomerates of hydrophobic CSD are therefore easily broken up and reach their final size and optimum distribution already under gentle mixing conditions (M1), while higher energies (M2) are required to break up agglomerates of hydrophilic CSD and to achieve an uniform coverage.

Adhesion Force Measurements

The adhesion force measurements between a MCC functionalized cantilever ("MCC-probe") and MCC–CSD mixtures or bulk MCC were performed with AEROSIL® 200, AEROSIL® 200 VV, and AEROSIL® R 972 V.

A typical plot of an individual measurement cycle is presented in Figure 4. To be sure that the MCC functionalized cantilever remained uncontaminated and intact during the course of the experiments, the particle integrity was examined under an optical microscope after each measurement cycle and the 300–500 values from each single run were evaluated in order to ascertain whether a systematic increase or decrease due to a change in the surface of the MCC probe had occurred. For all experiments, there was no systematic time dependent variation between single values within a run and the optical observation indicated no change of the MCC probe surface.

The cumulative distributions Q_0 of the adhesion forces are depicted in Figure 5. The curves represent the cumulative experimental measurements standardized to 1 for each sample. Each distribution indicates a non normal distribution. To characterize the samples, the mean, the standard deviation, and the standard error of the mean were calculated. Furthermore, the different samples were compared using a nonparametric

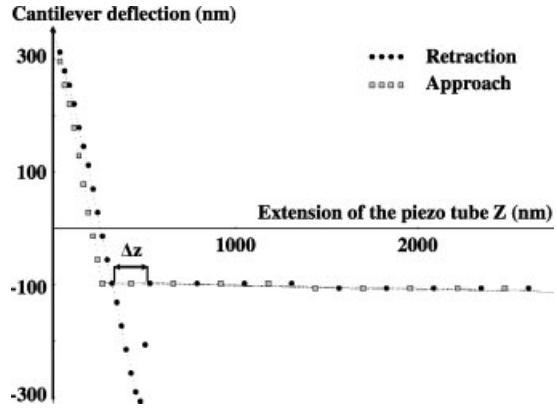

Figure 4. Illustration of the measurement of deflection of the cantilever versus the extension of the piezo tube of an individual adhesion measurement between a MCC functionalized cantilever and MCC containing 0.5% AEROSIL® 200.

Kruskal–Wallis or H-test followed by a Dunn's comparison test[36] (Table 3).

The cumulative frequencies, means, and non-parametric statistical test results showed that CSD reduced the adhesion force between the MCC

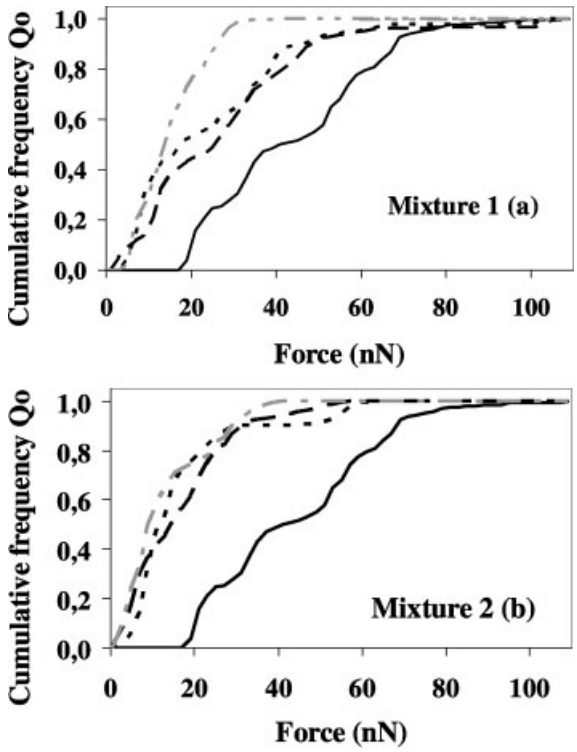

Figure 5. Cumulative adhesion forces between a MCC particle attached to the cantilever and bulk MCC (—) or MCC containing 0.5% AEROSIL® 200 (···), 5% AEROSIL® 200 VV (--), 0.5% AEROSIL® R 972 V (-·-) for mixtures M1 (a) and mixtures M2 (b).

functionalized cantilever and the MCC sample. This corroborates with the sandwich contacting system that describes the position of a small particle between two larger spheres—in our system CSD between two MCC particles. The smaller glidant particle increases the distance between the two larger excipient particles and the van der Waals forces between them are reduced.[37]

Under mixing conditions 1, adhesion forces obtained with MCC without CSD or with AEROSIL® 200, AEROSIL® 200 VV, and AEROSIL® R 972 V ranged from 18 to 110 nN, from 2 to 106 nN, from 2 to 110 nN, and from 2 to 40 nN, respectively. Differences in adhesion between individual sites were expected for MCC and could be explained by the matchstick-like or rod-like structure of MCC.[38] Through this structure, the number of contact points between the MCC particle mounted to the cantilever and the sample varied from one site to the other, leading to a large adhesion force range. This situation is depicted in Figure 6a. Mixtures M1 containing either compacted or non-compacted hydrophilic CSD showed no statistically significant differences in their adhesion means. The means were smaller compared to pure MCC, as expected, but the range of adhesion was still high. This observation can be attributed to the degree of coverage of CSD on MCC. SEM analysis revealed that the surface of the MCC was not completely covered by hydrophilic CSD under mixing conditions 1. Consequently, during the measurement, the cantilever can reach a MCC surface either without, with few, or with many CSD particles as depicted schematically by Figure 6b. These various contact point possibilities resulted in a wide range of adhesion forces. By contrast, addition of 0.5% hydrophobic CSD led to a small range and statistically significant lower mean of the adhesion force. As shown by SEM images, the distribution of hydrophobic CSD on MCC was homogeneous after gentle mixing in the free-fall mixer. This homogeneous coverage allowed a MCC–CSD–MCC contact (Fig. 6c), which led to a smaller adhesion force mean and a smaller range of the adhesion force compared to the sample M1 containing hydrophilic CSD.

Through additional mixing in the high speed mixer (M2), the mean, the standard deviation, and the range of the adhesion force decreased for mixtures containing hydrophilic CSD. The smaller range of the adhesion force distribution, from 1 to 74 nN and from 1 to 60 nN for AEROSIL® 200 and AEROSIL® 200 VV, respectively, was attributed to a better distribution of the CSD, as

Table 3. Means, Standard Deviations (SD), Standard Errors (SE), and Number of Measurements of the Adhesion Force Distributions

		Mixture 1			Mixture 2		
	MCC	AEROSIL® 200	AEROSIL® 200 VV	AEROSIL® R 972 V	AEROSIL® 200	AEROSIL® 200 VV	AEROSIL® R 972 V
Mean (nN)	44.8	25.2	28.4	13.9	17.5	17.4	13.8
SD (nN)	19.3	19.8	20.9	7.4	14.1	8.7	9.9
SE (nN)	1.2	0.9	0.9	0.3	0.6	0.4	0.4
n	254	536	600	485	543	572	596

observed by SEM images (Fig. 3d,f). Schematically, the measurements under mixing conditions 2 could be described by Figure 6c. In this case primarily MCC–CSD–MCC contact occurred. Consequently, the means for both samples M2 were statistically significant smaller compared to M1 and approached the mean of sample M2 with hydrophobic CSD. Mixtures M1 and M2 containing hydrophobic CSD presented no statistically significant differences in adhesion force means and showed nearly the same curve shape and range of adhesion force distribution, as they already presented the same degree and uniformity of coverage. This observation indicated that adhesion force was dependent on the degree and uniformity of coverage of the CSD on the MCC surface.

Correlation between Angle of Prepose and Adhesion Force

As shown in Figure 7, the correlation between the angle of repose and the adhesion force mean was linear. The smaller the angle of repose, the smaller the adhesion between the MCC particle affixed to the cantilever and the sample surface. The measurement of the angle of repose explains the global and effective action of the CSD on MCC. AFM allowed the characterization of the glidant action on an MCC particle-to-particle contact level. The adhesion force measurement performed by AFM was not the absolute adhesion force, because the area of each sampling point was unknown.[25] The mean of the distribution was calculated, the adhesion measurements of each sample were statistically compared and the results represented best the phenomena within the powder mixtures. Both methods, namely the angle of repose and AFM, showed that the glidant properties depended on the nature of the CSD and the mixing conditions.

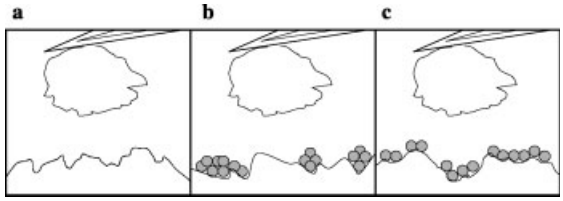

Figure 6. Schematic representation of three contact possibilities between the MCC functionalized tip and the MCC sample during the adhesion free measurement, focusing on the coverage of MCC sample by CSD types: (a) MCC–MCC contact; (b) MCC–MCC or/and MCC–CSD–MCC contact; and (c) MCC–CSD–MCC contact.

CONCLUSION

The angle of repose of MCC as a measure of its flow properties was reduced, depending on the mixing conditions, from 47° to between 38 and 40°

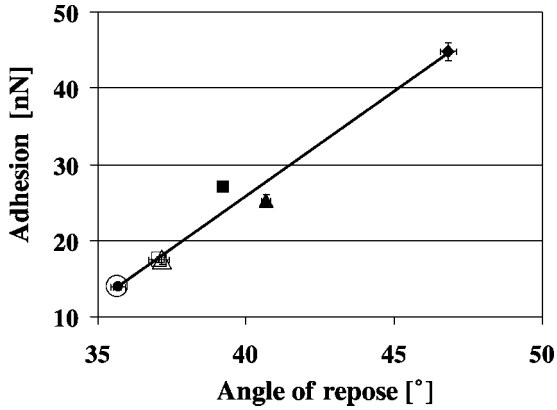

Figure 7. Correlation between the angle of repose and the adhesion force mean of MCC containing 0.5% AEROSIL® R 972 V [M1, (●) M2, (○)], 0.5% AEROSIL® 200 [M1, (■); M2, (□)], 0.5% AEROSIL® 200 VV [M1, (▲); M2, (△)], and MCC as bulk (◆). Error bars indicate the standard error (SE) of the mean.

by the addition of different hydrophilic CSD types. Hydrophobic CSD resulted in a reduction to 36° independent of the mixing conditions. This macroscopic effect supported by bulk and tapped densities could be verified by SEM images and AFM measurements. SEM images showed a uniform distribution of hydrophobic CSD particles on the MCC surface even under gentle mixing conditions while for hydrophilic CSD stronger mixing conditions were required. The AFM measurements resulted in an adhesion force reduction of the mean from 44.8 nN for pure MCC to at least 17.5 nN for hydrophilic and 13.9 nN for hydrophobic CSD, the latter being independent from the mixing conditions. In addition the adhesion force variation was lower with hydrophobic CSD. A linear correlation between the angle of repose and the adhesion force was established. These results indicate that hydrophobic CSD has some advantages in powder mixing compared to the hydrophilic type. For routine measurements the angle of repose is a sufficient method to compare different types of flow enhancing substances.

ACKNOWLEDGMENTS

This work was supported by Degussa AG (Hanau, Germany). The authors thank Ms. Maribel De la Garza from the Chair of Particle Technology of TU-Munich for her assistance with the AFM and the Chair of Process Engineering of Disperse Systems TU-Munich for helpful advices.

REFERENCES

1. Egermann H, Frank P. 1990. Novel approach to estimate quality of binary random powder mixtures: Samples of constant volume. II—Applications of equation to optimize tableting conditions. J Pharm Sci 81:667–669.
2. Kornchankul W, Hamed E, Parikh N, Sakr A. 2002. Effect of the drug proportion and mixing time on the content uniformity of a low dose drug in a high shear mixer. Pharmazie 57:49–53.
3. Otsuka M, Gao J, Matsuda Y. 1993. Effects of mixer and mixing time on the pharmaceutical properties of theophilline tablets containing various kinds of lactose as diluents. Drug Dev Ind Pharm 19:333–348.
4. Schweiger A, Sindel U, Zimmermann I. 1997. Determination of the optimum mixing time for a mixture of lactose and corn starch. Pharm Ind 59:985–988.
5. De Villiers M, Van der Watt J. 1994. The measurement of mixture homogeneity and dissolution to predict the degree of drug agglomerate breakdown achieved through powder mixing. Pharma Res 11: 1557–1661.
6. Poux M, Fayolle P, Bertrand J. 1991. Powder mixing: Some practical rules applied to agitated systems. Powder Technol 68:213–234.
7. Egermann H. 1976. Contributions to the technological behaviour of glidants. 1. The effects of the time of mixing of glidants on the packing properties of direct-tablet table adjuvants. Scientia Pharmaceutica 44:81–93.
8. Swaminathan V, Kildsig D. 2002. Effect of the magnesium stearate on the content uniformity of active ingredient in pharmaceutical powder mixtures. AAPS Pharm Sci Tech 3(3). Article 19. [http://www.aapspharmscitech.org]
9. Sindel U, Schweiger A, Zimmermann I. 1998. Determination of the optimum mixing time for a mixture of lactose and colloidal silicon dioxide. J Pharm Sci 87(4):524–526.
10. Ullrich WJ. 1998. Powder flow measurement techniques what's new? Adv Powder Metallur Particulate Mater 1:107–127.
11. Amidon GE, Ausburger LL, Brittain HG, Byrn SR, Fox CD, Peck GE, Wurster DE. 1999. Physical test methods for powder flow characterization of pharmaceutical materials: A review of methods. Pharmacopeial Forum 25(3):8298–8308.
12. Nikolakakis I, Ballesteros Aragon O, Malamataris S. 1998. Resistance to densification, tensile strength, and capsule-filling performance of some pharmaceutical diluents. J Pharm Pharmacol 50: 713–721.
13. Podczeck F. 1998. Particle–particle adhesion in pharmaceutical powder handling. London: Imperial College Press, pp 141–159.
14. Binning G, Quate CF, Gerber C. 1986. Atomic force microscope. Phys Rew Lett 56:930–933.
15. Louey MD, Mulvaney P, Stewart PJ. 2001. Characterisation of adhesional properties of lactose carriers using atomic force microscopy. J Pharm Anal 25:559–567.
16. Giessibl FJ. 2003. Advances in atomic force microscopy. Rew Mod Phys 75:949–983.
17. Finot E, Lesniewska E, Mutin JC, Goudonnet JP. 1999. Investigations of surface forces between gypsum crystals in electrolytic solutions using microcantilevers. J Chem Phys 111:6590–6598.
18. Mueller H, Butt HJ, Bamberg E. 1999. Force measurements on myelin basic protein adsorbed to mica and lipid bilayer surfaces done with atomic force microscope. Biophys J 76:1072–1079.
19. Gillies G, Prestidge CA, Attard P. 2002. An AFM study on the deformation and nanorheology of cross-linked PDMS droplets. Langmuir 18:1674–1679.
20. Agache V, Legrand B, Collard D, Buchaillot L. 2002. Adhesive forces investigation on a silicon tip by contact-mode atomic force microscope. Appl Adv Phys 81:2623–2625.

21. Sindel U, Zimmermann I. 2001. Measurement of interaction forces between individual powder particles using an atomic force microscopy. Powder Technol 117:247–254.
22. Heng PWS, Chan LW, Lim LT. 2000. Quantification of the surface morphologies of lactose carriers and their effect on the *in vitro* deposition of salbutamol sulphate. Chem Pharm Bull 48:393–398.
23. Ibrahim TH, Burk TR, Etzler FM, Neuman RD. 2000. Direct adhesion measurements of pharmaceutical particles to gelatine capsule surfaces. J Adhesion Sci Technol 14:1225–1242.
24. Begat P, Young P, Edge S, Kaerger J, Price R. 2003. The effect of mechanical processing on surface stability of pharmaceutical powders: Visualization by atomic force microscopy. J Pharm Sci 92:611–620.
25. Eve JK, Patel N, Luk SY, Ebbens SJ, Roberts CJ. 2002. A study of single drug particle adhesion interactions using atomic force microscopy. Int J Pharm 232:213–224.
26. Young PM, Price R, Tobyn MJ, Buttrum M, Dey F. 2003. Investigation into the effect of humidity on drug–drug interactions using the atomic force microscope. J Pharm Sci 92:815–822.
27. Bérard V, Lesniewska E, Andrès C, Pertuy D, Laroche C, Pourcelot Y. 2002. Dry powder inhaler: Influence of humidity on topology and adhesion studied by AFM. Int J Pharm 232:213–224.
28. Wang J, Li T, Bateman S, Erck R, Morris K. 2003. Modeling of adhesion in tablet compression-I. Atomic force microscopy and molecular simulation. J Pharm Sci 92:798–814.
29. Ohta KM, Fuji M, Chikazawa M. 2003. Effect of geometric structure of flow promoting agents on the flow properties of pharmaceutical powder mixture. Pharm Res 20:804–809.
30. Weth M, Hofmann M, Kuhn J, Fricke J. Measurement of attractive forces between single aerogel powder particles and the correlation with powder flow. J Non Crystalline Solids 285:236–243.
31. Degussa AG. 1993. Schriftenreihe Pigmente No. 11, "Grundlagen von AEROSIL®". 5th Edn, Frankfurt: Author, pp 17, 78–79.
32. Cleveland JP, Manne S, Bocek D, Hansma PK. 1993. A non-destructive method for determining the spring constant of cantilevers for scanning force microscopy. Rev Sci Instrum 64:403–405.
33. Maganov SN, Whangbo M-H. 1996. Surface analysis with STM and AFM. Weinheim: VCH Verlagsgesellschaft mbH, pp 12–13.
34. Willing GA, Ibrahim TH, Etzler FM, Neuman RD. 2000. New approach to the study of particle–surface adhesion using atomic force microscopy. J Colloid Interface Sci 226:185–188.
35. Jonat S, Hasenzahl S, Drechsler M, Albers P, Wagner KG, Schmidt PC. 2004. Investigation of compacted hydrophilic and hydrophobic colloidal silicon dioxides as glidants for pharmaceutical excipients. Powder Technol 141:31–43.
36. Sachs L. 2002. Angewandte Statistik. 11. Auflage. Berlin, New York, Heidelberg: Springer-Verlag, pp 394–401.
37. Xie H-Y. 1997. The role of interparticle forces in the fluidization of fine particles. Powder Technol 94: 99–108.
38. Bolhuis G, Chowan Z. 1996. Materials for direct compaction. In: Alderborn G, Nyström C, editors. Pharmaceutical powder compaction technology. New York, Basel: Marcel Dekker, pp 428–440.